J Appl Electrochem (2009) 39:1597–1602
DOI 10.1007/s10800-009-9848-8

ORIGINAL PAPER

Improving electrochemical performance of NiO films by electrodeposition on foam nickel substrates

Hongbo Wang · Qinmin Pan · Xiaopeng Wang · Geping Yin · Jianwei Zhao

Received: 1 August 2008 / Accepted: 18 February 2009 / Published online: 1 March 2009

Abstract NiO films for lithium-ion batteries were deposited on copper plates and foam nickel substrates by electrodeposition and subsequent heat treatment at 300 °C. At a discharge/charge rate of 0.1 C, foam NiO films delivered reversible capacity larger than 650 mAh g^{-1} and capacity retention over 93% after 50 cycles. NiO films deposited on foam nickel exhibited higher reversible capacity, better cyclability, as well as higher rate capability than those on copper plates. The unique three-dimensionally porous morphologies of foam NiO films were responsible for the better electrochemical performance, which provided not only high electrode/electrolyte contact area but also a good electronic conduction matrix. The present finding offers a new pathway for the large scale fabrication of high-energy-density electrodes for lithium-ion batteries.

Keywords NiO films · Electrodeposition · Foam nickel substrates · Electrochemical performance · Lithium-ion batteries

1 Introduction

As a novel kind of anode material for lithium-ion batteries, transition metal oxides MO (such as CoO, NiO, Co_3O_4 and CuO, etc.) have been intensively investigated in the past few years owing to their high theoretical capacities and good safety [1, 2]. Generally, these MO materials exhibit a different lithium storage mechanism from conventional carbonaceous materials, which can be illustrated by the following equations.

$$MO + 2Li^+ + 2e^- \leftrightarrow M + Li_2O$$

$$xM + yLi \leftrightarrow M_xLi_y$$

It is now well established that morphology and crystallinity are important factors that affect the electrochemical properties of MO anodes [3, 4].

Among a variety of MO materials, NiO has a high theoretic capacity of 718 mAh g^{-1} when used as anode materials for lithium-ion batteries [5, 6]. However, the reversible capacity and cycling characteristics of NiO are worse than those of other transition metal oxides; this arises from the low electronic conductivity and large volume change of NiO particles in the process of lithium insertion/extraction. To overcome these problems, preparing nanostructured materials was shown to be an effective solution because nanomaterials facilitate the transportation of Li ions and electrons, and alleviate the volume change of active particles [7–9]. In addition, fabricating composite materials is another method to improve the electrochemical performance of MO materials [10–12].

Recently, fabricating porous film-electrodes on foam nickel substrates has provided an alternative approach to improve the reversible capacity and rate capability of MO anodes [13, 14]. For example, Chen et al. [15, 16] demonstrated that foam-nickel-supported Cu_2O and CoO showed excellent electrochemical performance in lithium-ion batteries. Moreover, highly porous NiO/Ag films constructed by chemical bath deposition also exhibited desirable electrochemical behavior [17]. Nevertheless, the

H. Wang · Q. Pan (✉) · X. Wang · G. Yin
School of Chemical Engineering and Technology,
Harbin Institute of Technology, 150001 Harbin,
People's Republic of China
e-mail: panqm@hit.edu.cn

J. Zhao
School of Chemistry and Chemical Engineering, Nanjing
University, 210023 Nanjing, People's Republic of China

preparation of these porous MO films involved either complicated equipment or very low utilization of raw materials (e.g. chemical bath deposition). Therefore, a straightforward and highly efficient process for fabricating MO film on foam nickel substrates is required.

In this study, we prepare NiO films on copper plates and foam nickel substrates via electrodeposition followed by heat treatment at moderate temperature. We demonstrate here that the NiO films deposited on foam nickel exhibit higher reversible capacity, better cyclability and rate capability than those on copper plates. Compared to the methods reported previously, the procedure described here has the advantages of ready availability of reagents and equipment, convenience, high efficiency and low cost.

2 Experimental

Foam nickel plates used in this study had a BET surface area of 0.39 $m^2\ g^{-1}$, porosity of 86.8%, thickness of 1.6 mm, and pore size of 500 μm. The foam nickel plates were pressed into a thickness of about 30 μm before the deposition. In a typical experiment, foam nickel and copper plates (4 cm × 2 cm) were successively washed with 1.0 M HCl and deionized water to remove surface impurities. Then the plates were put in a bath containing 0.18 M $Ni(NO_3)_2$ solution at 90 °C and acted as the working electrodes. A pure nickel sheet was used as the active anode. Galvanostatic electrodeposition was carried out at a current of 20 mA for 40 min. After being rinsed with water, the resulting plates were heated at 300 °C for 30 min in a quartz-tube under argon atmosphere. The NiO films deposited on copper plates and foam nickel substrates were are termed planar-NiO and foam-NiO, respectively.

The NiO films were cut into 1.1 cm^2 circular plates, and then dried in vacuum and weighed. Lithium foils were used as the counter and reference electrodes. The electrolyte was 1.0 M $LiPF_6$ in EC/DMC (1:1 by volume). Coin cells were assembled in a glove-box under argon atmosphere. The electrochemical performance of the NiO films was evaluated by galvanostatic discharge (lithium insertion)/charge (lithium extraction) measurement using a computer-controlled battery tester between 0 and 3.0 V. Cyclic voltammograms (CVs) were recorded on a CHI604 potentiostat at a scan rate of 0.5 mV s^{-1}. All the potentials indicated here are referred to the Li/Li^+ electrode.

The mass of NiO films was estimated to be about 3.0 mg cm^{-2} according to the procedure described in [18]. Scanning electron microscopy (SEM) images and energy dispersive X-ray analysis (EDX) were obtained with a QUANTA200 (FEI) scanning electron microscope. X-ray diffraction (XRD) analysis was carried out on a Philips PW-1830 instrument.

3 Results and discussion

Figure 1 shows the SEM images of foam-NiO and planar-NiO films. The films show fractured appearances composed of platelets a few micrometers in size. For foam-NiO, the platelets display porous morphologies with pore sizes of about 200 nm (Fig. 1c), indicating the presence of binary structures on both micro- and nanometer scales. The thickness of these platelets is about 2.0 μm (Fig. 1c). In contrast, the platelets on planar-NiO exhibit clear and smooth surfaces, and almost no pores are observed. As seen from Fig. 1, the film deposited on copper is thicker than that on foam nickel. It is reasonable that the foam-NiO films have very high electrode/electrolyte contact area as the anodes of lithium-ion batteries. Figure 2 displays the SEM images of unheated films deposited on copper plates and foam nickel substrates. The unheated films exhibit larger platelets but narrower cracks compared to the images in Fig. 1.

The chemical composition and crystal structure of the NiO films were confirmed by XRD and EDX, as shown in Fig. 3. All the diffraction peaks in Fig. 3a can be ascribed to cubic NiO and no impurity is observed, indicating the existence of NiO film on copper plates. EDX measurement also ascertains the presence of NiO film on foam nickel substrates. The formation mechanism of NiO films can be illustrated by the following equations [19].

$$Ni(NO_3)_2 \rightarrow Ni^{2+} + 2NO_3^- \quad (1)$$

$$NO_3^- + H_2O + 2e^- \rightarrow 2OH^- + NO_2^- \quad (2)$$

$$Ni^{2+} + 2OH^- \rightarrow Ni(OH)_2 \quad (3)$$

$$Ni(OH)_2 \rightarrow NiO + H_2O \quad (4)$$

Figure 4 shows the cyclic voltammograms of these NiO films in the potential range 0–3.0 V at a rate of 0.5 mV s^{-1}. In the first discharge scan, there are two cathodic peaks at 1.0 V and 0.25 V for planar-NiO, while only one strong cathodic peak is observed at 0.18 V for foam-NiO. The cathodic peaks correspond to the reduction of NiO into Ni, and the formation of solid electrolyte interface (SEI), respectively [20]. As for foam-NiO, the potentials of these reactions are so close that they overlap into a strong peak. For both kinds of NiO film, there are two anodic peaks located at about 1.75 V and 2.30 V in the first scan, which can be assigned to the decomposition of SEI and the reaction between Ni and Li_2O, respectively [21]. Compared to planar-NiO, however, foam-NiO exhibits a stronger peak at 1.75 V. A possible explanation for this difference is the catalytic decomposition of Li_2O on foam nickel substrates during charging, because a similar phenomenon was also observed in Ni-coated ZnO [22].

The voltage profiles of the NiO films at 0.1 C (1 C = 718 mA g^{-1}) are shown in Fig. 5. Each film

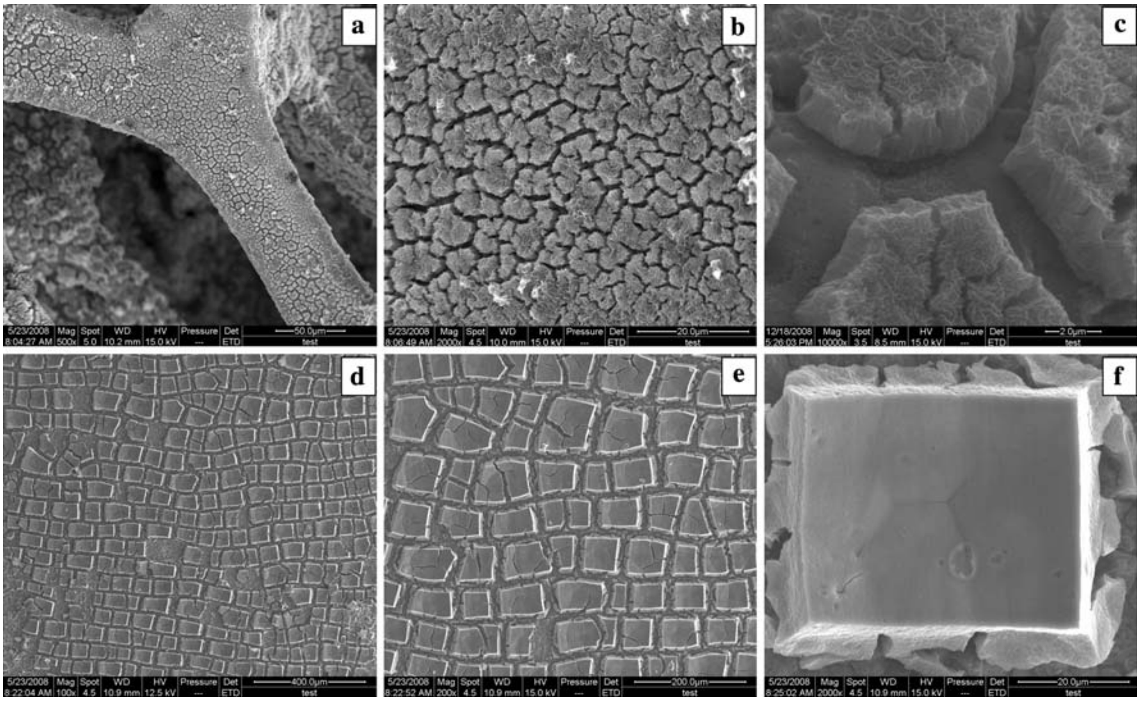

Fig. 1 SEM images of NiO films deposited on foam nickel (**a–c**) and copper plates (**d–f**)

Fig. 2 SEM images of precursor films on foam nickel (**a**) and copper plate (**b**) substrates without heat treatment

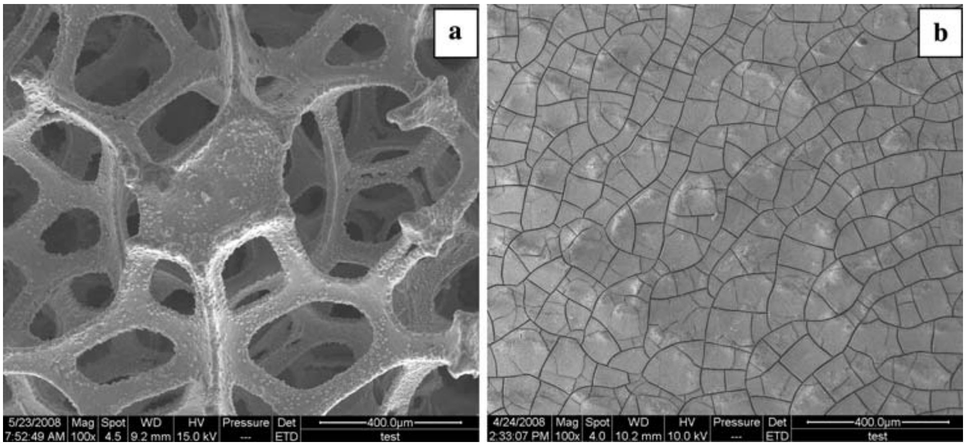

exhibits a long voltage plateau at about 0.75 V followed by a sloping curve during the first discharge. This plateau disappears in the subsequent discharge process, suggesting a heterogeneous reaction mechanism of lithium insertion and extraction. In the lithium extraction process, there are two plateaux on the charge curves. The first discharge process delivers a capacity of 990 mAh g^{-1} for foam-NiO and 1110 mAh g^{-1} for planar-NiO. Both values are larger than the theoretical capacity of NiO (718 mAh g^{-1}), due to the decomposition of electrolyte components and subsequent formation of solid electrolyte interface on the surface of NiO particles [23, 24]. Nevertheless, foam-NiO exhibits higher charge capacity (689 mAh g^{-1}) than planar-NiO (583 mAh g^{-1}). Therefore, foam-NiO shows a higher initial coulombic efficiency (68.7%) than planar-NiO (52.5%).

Figure 6 presents the cycling characteristics of the two kinds of NiO films at 0.11 C. After discharge/charge for 50 cycles, foam-NiO retains 93.2% of its initial capacity of 651 mAh g^{-1}, while that of planar-NiO is only 55.1% (322 mAh g^{-1}). Moreover, foam-NiO also exhibits better rate capability than planar-NiO, and charge capacity as a function of rate is plotted in Fig. 7. On the whole, capacity decreases as discharge-charge rate increases. However, the capacity of planar-NiO drops more rapidly than that of foam-NiO. At a rate of 1.0 C, only 47 mAh g^{-1} is obtained for planar-NiO, while foam-NiO is able to retain a capacity over 300 mAh g^{-1}, suggesting that foam-NiO favors high-

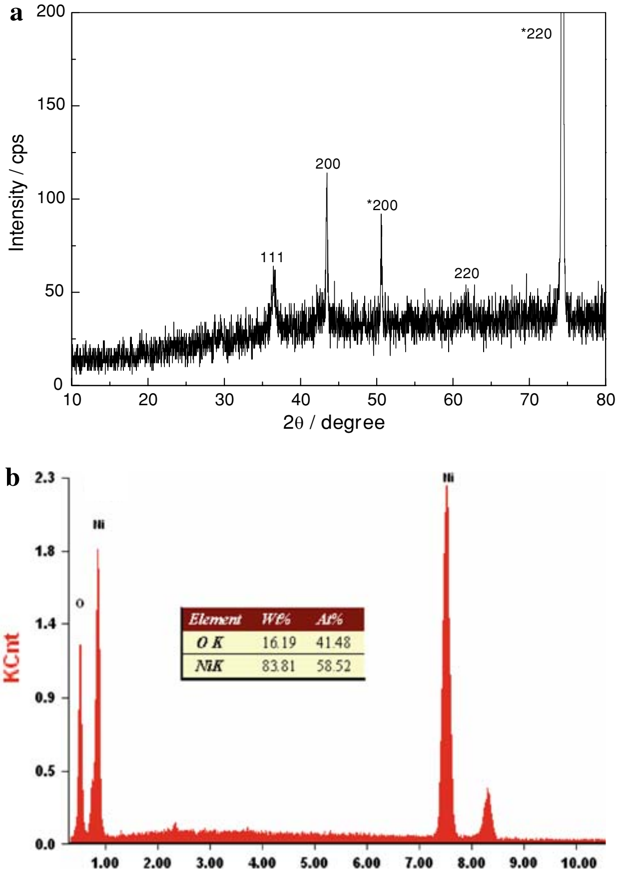

Fig. 3 XRD pattern (**a**) and EDX plot (**b**) of NiO films deposited on copper plate and foam nickel substrate, respectively

rate charge transportation. This is a very desirable feature for battery electrodes where fast-rate discharge-charge capability is required. For the purpose of comparison, we compared the performance with previously reported NiO [5, 6, 17, 20, 21, 23–25]. It is found that the previously reported NiO exhibited lower reversible capacity and/or poor cyclability compared to foam-NiO. Two comparable cases were reported by Zhou et al. [14, 26]. It should be noted that though a three-dimensionally porous structure may improve the fast-rate performance, it may also decrease the volume capacity of lithium-ion batteries. However, the reversible capacity of foam-NiO is approximately twice that of commercial graphite electrodes. This high capacity compensates the decreased volume capacity caused by the porous structure. Furthermore, the thickness of foam-NiO films used in this study is about 35 μm, which is close to that of commercial graphite electrodes. Therefore, the volume capacity decrease due to the porous structure will be limited compared to commercial graphite electrodes.

The difference in the performance of the two kinds of NiO films can be explained by impedance spectra, as shown in Fig. 8. Compared to planar-NiO, foam-NiO displays a smaller semicircle in the medium frequency region, indicating a lower charge transfer resistance. It is well known that NiO particles and the SEI formed on its surface are poor electronic conductors. Consequently, the electrochemical behavior of NiO electrodes is significantly affected by the electrical contact of NiO particles. For foam-NiO, nickel foam substrate forms an excellent conduction network for NiO particles, which guarantees the electronic kinetics at the electrode/electrolyte interface. Secondly, the three-dimensionally porous structure has very high electrode/electrolyte contact area, favoring fast transport of lithium ions and electrons [27, 28]. In addition, the porous microstructure also provides sufficient space to buffer the volume change of NiO particles during lithium insertion-extraction. As a result, foam-NiO possesses larger reversible capacity, better cyclability and higher rate capability than its planar-NiO counterpart.

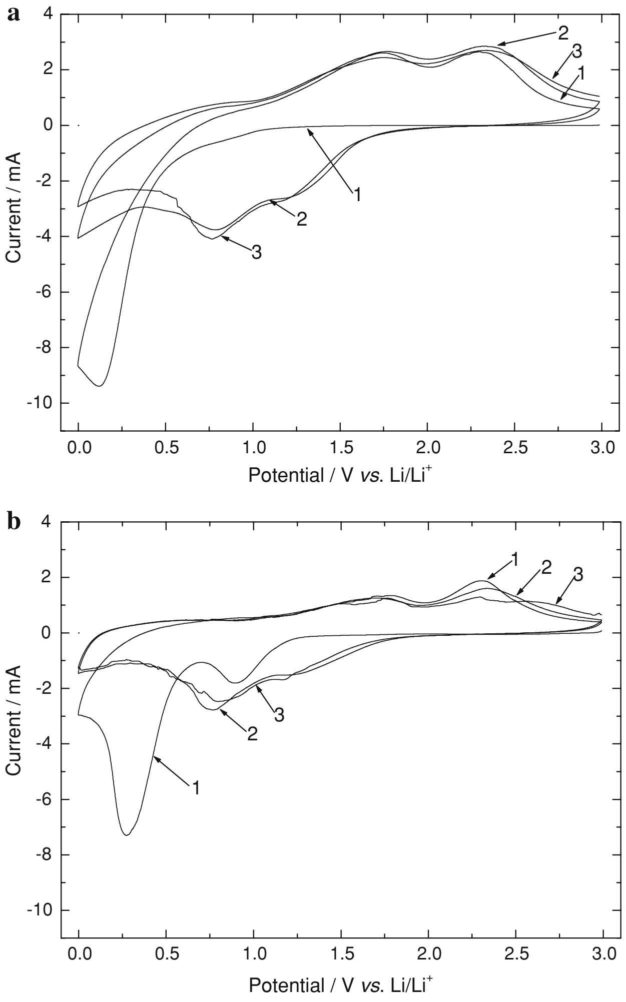

Fig. 4 Cyclic voltammograms of foam-NiO (**a**) and planar-NiO (**b**) films at a scan rate of 0.5 mV s^{-1}

We also found that the electrodeposition time played an important role in the electrochemical properties of NiO

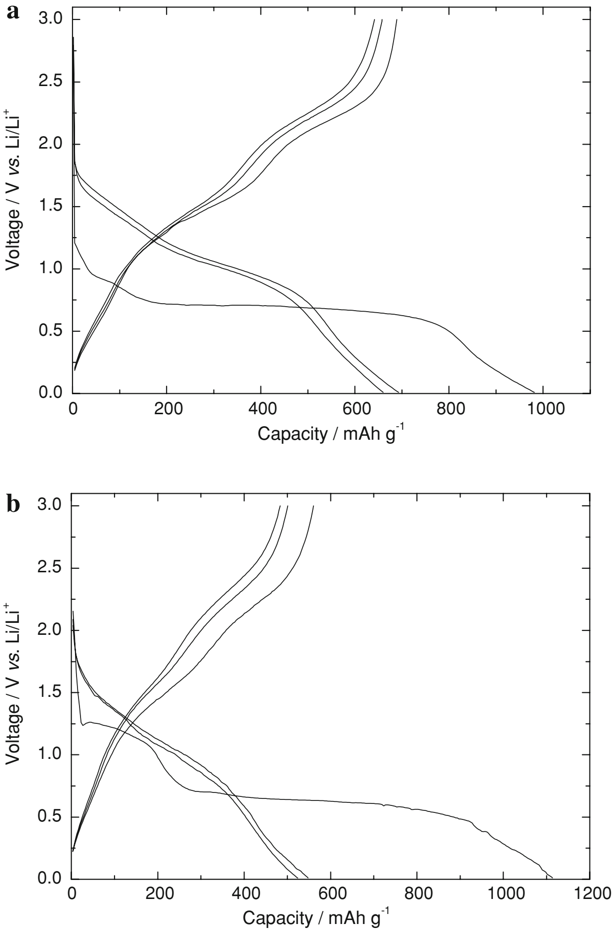

Fig. 5 Voltage profiles of foam-NiO (**a**) and planar-NiO (**b**) films at a rate of 0.10 C

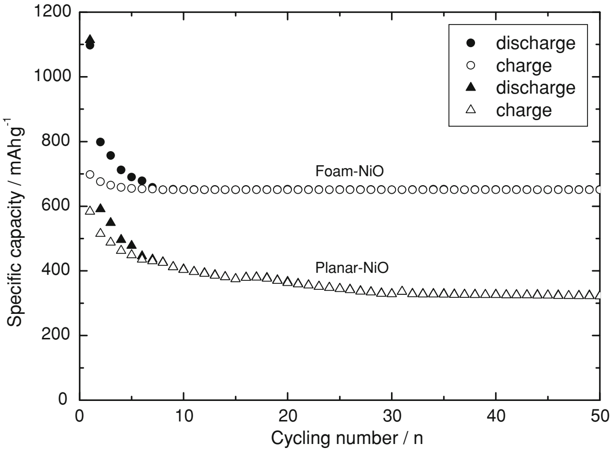

Fig. 6 Cycling performance of NiO films at a rate of 0.11 C

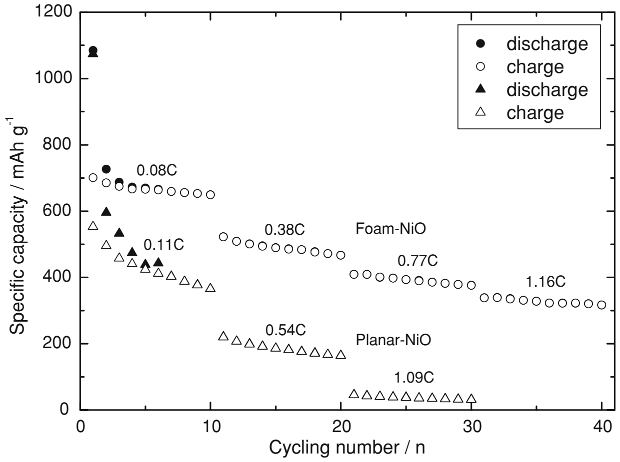

Fig. 7 Dependence of capacities of NiO films on discharge-charge rate

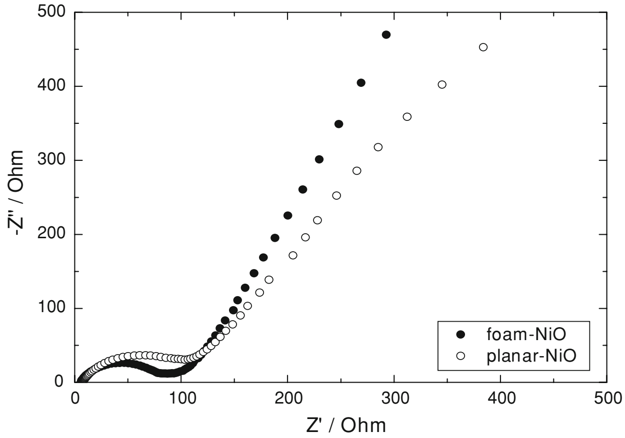

Fig. 8 Electrochemical impedance spectra of NiO films at open circuit voltage

films. The discharge capacities of the films deposited for different time are summarized in Fig. 9. For both kinds of NiO film, shortening the deposition time favours higher discharge capacity, better cyclability and even higher rate capability, indicating that the thickness of NiO layers exerts an important influence on electrochemical performance. Since NiO is a poor semiconductor and the NiO films in this study are without conducting agent, the charge transfer process within NiO films is strongly affected by the distance between the NiO particles and the current collector. Charge transfer is easier for the particles nearer to the current collector than it is for the outer ones [29, 30].

4 Conclusions

In summary, NiO films for lithium-ion batteries were deposited on copper plates and foam-nickel substrates via cathodic electrodeposition and subsequent heat treatment at moderate temperature. The films deposited on foam nickel substrates exhibited better electrochemical performance, including higher reversible capacity, better cyclability and rate capability, than those on copper plates. It is believed

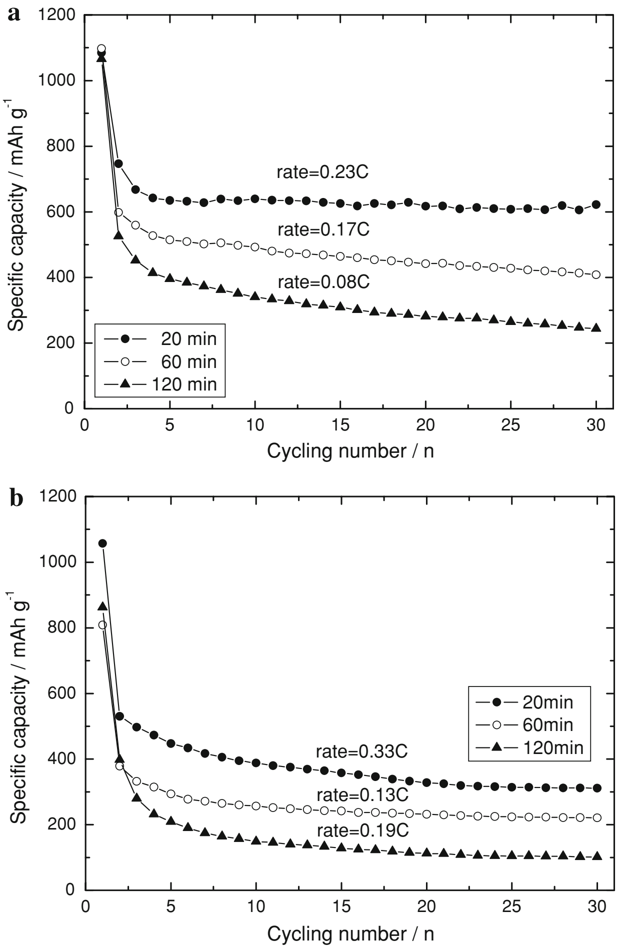

Fig. 9 Effect of electrodeposition time in Ni(NO$_3$)$_2$ solution on the discharge capacities of foam-NiO (**a**) and planar-NiO (**b**) films

that the better electrochemical properties of foam-NiO films originates from their highly porous morphologies. Since the electrochemical method reported here has the advantages of easy control, environmental compatibility and convenience; the present finding opens the possibility to produce high-energy-density electrodes for power sources on large scale.

Acknowledgement This work was supported by Natural science foundation of China (Grant No. 50803013).

References

1. Poizot P, Laruelle S, Grugeon S, Dupont L, Tarascon JM (2000) Nature 407:496
2. Arico S, Peter B, Bruno S, Tarascon JM, Schalkwijk WV (2005) Nat Mater 4:366
3. Wang SQ, Zhang JY, Chen CH (2007) Scr Mater 57:337
4. Gao XP, Bao JL, Pan GL, Zhu HY, Huang PX, Wu F, Song DY (2004) J Phys Chem B 108:5547
5. Li YG, Tan B, Wu YY (2008) Chem Mater 20:567
6. Oh SW, Bang HJ, Bae YC (2007) J Power Source 173:502
7. Needham SA, Wang GX, Liu HK (2006) J Power Source 159:254
8. Wang X, Li L, Zhang YG (2006) Cryst Growth Des 6:2163
9. Yuan L, Guo ZP, Konstantinov K (2006) Electrochem Solid State Lett 9:A524
10. Huang XH, Tu JP, Zhang CQ, Chen XT, Yuan YF, Wu HM (2007) Electrochim Acta 52:4177
11. Huang XH, Tu JP, Zhang CQ, Xiang JY (2007) Electrochem Commun 9:1180
12. Yoshio I, Tadahiko K, Akihiro M, Yukio M, Tsutomu M (1997) Science 276:1395
13. Moriguchi I, Hidaka R, Yamada H, Kudo T, Murakami H, Nakashima N (2006) Adv Mater 18:69
14. Pan QM, Liu J (2008) J Solid State Electrochem. doi: 10.1007/s10008-008-0740-y
15. Yu Y, Chen CH, Shui JL, Xie S (2005) Angew Chem Int Ed 44:7085
16. Yu Y, Shi Y, Chen CH (2007) Nanotechnology 18:055706
17. Huang XH, Tu JP, Zeng ZY, Xiang JY, Zhao XB (2008) J Electrochem Soc 155:A438
18. Wang HB, Pan QM, Zhao JW, Yin GP, Zuo PJ (2007) J Power Sources 167:206
19. Izaki M, Omi T (1996) J Electrochem Soc 143:L53
20. Grugeon S, Laruelle S, Herrera-Urbina R, Dupont L, Poizot P, Tarascon JM (2001) J Electrochem Soc 148:A285
21. Debart A, Dupont L, Poizot P, Leriche JB, Tarascon JM (2001) J Electrochem Soc 148:A1266
22. Zhang CQ, Tu JP, Yuan YF, Huang XH, Chen XT, Mao F (2007) J Electrochem Soc 154:A65
23. Tarascon M, Morcrette M, Dupont L, Chabre Y, Payen C, Larcher D, Pralong VJ (2003) J Electrochem Soc 150:A732
24. Laruelle S, Grugeon S, Poizot P, Dolle M, Dupont L, Tarascon JM (2002) J Electrochem Soc 149:A627
25. Huang XH, Tu JP, Xia XH, Wang XL, Xiang JY (2008) Electrochem Commun 10:1288
26. Hosono E, Fujihara S, Honma I, Zhou H (2006) Electrochem Commun 8:284
27. Martin CR, Mitchell DT (1999) Electroanal Chem 21:1
28. Sorensen EM, Barry SJ, Jung HK, Rondinelli JR, Vaughey JT, Poeppelmeier KR (2006) Chem Mater 18:482
29. Sauvage F, Baudrin E, Gengembre L, Tarascon JM (2005) Solid State Ion 176:1869
30. Pan QM, Wang M (2008) J Electrochem Soc 155:A452